Eur. Phys. J. B **7**, 533–540 (1999)

THE EUROPEAN PHYSICAL JOURNAL B
EDP Sciences

Anomalous magnetic behavior of superconducting $Tl_2Ba_2CaCu_2O_8$ thin films in small magnetic fields close to the transition temperature

H.A. Radovan[1], H.H. Wen[1,2], and P. Ziemann[1,a]

[1] Abteilung Festkörperphysik, Universität Ulm, 89069 Ulm, Germany
[2] National Laboratory for Superconductivity, Institute of Physics and Center for Condensed Matter Physics, P.O. Box 603, Beijing 100080, P.R. China

Received: 8 April 1998 / Revised: 15 July 1998 / Accepted: 2 September 1998

Abstract. Using a specially designed SQUID magnetometer we measured the temperature dependence of the critical current density in a ring patterned $Tl_2Ba_2CaCu_2O_8$ thin film for magnetic fields 0.03 Oe $\leq H <$ 30 Oe parallel to the c-axis. In addition, the temporal relaxation of the remanent state as prepared by field cooling in an external field of 100 Oe at different temperatures $T \leq 93$ K $< T_c$ is determined. The $j_c(T)$ data show a field-dependent anomalous kink close to T_c pointing to reduced dissipation with increasing temperature allowing to construct a corresponding H-T borderline. A similar behavior is observed for the normalized relaxation rate $S(T)$ as extracted from the temporal behavior of the remanent state, which, at low temperatures, exhibits the expected increase for increasing T-values, while an anomalous decrease of $S(T)$ is found for temperatures above 85 K. While the low-T regime is attributed to creep of 2D pinned single vortex lines, the high-T behavior is suggested to be dominated by collective motion with a more sluggish dynamics. This change in dynamics is also reflected by the activation barriers for flux creep $U(j)$, which show a corresponding crossover in μ from 0.06 to 0.99. An additional scaling analysis of the E-j characteristics for $T \geq 85$ K according to vortex glass theory reveals quasi-2D collective creep behavior with $T_g = 96$ K.

PACS. 74.60.Ge Flux pinning, flux creep, and flux-line lattice dynamics – 74.76.Bz High-T_c films – 74.25.Dw Superconductivity phase diagrams

1 Introduction

Ever since the discovery of the high-T_c superconductors (HTSC), the H-T vortex phase diagram has been a subject of intense experimental and theoretical investigations. This is especially true for the most structurally anisotropic HTSC families of which $Tl_2Ba_2CaCu_2O_8$ is a representative example. In these systems with a pronounced layered structure, a subtle interplay is observed between the thermal energy and intralayer as well as interlayer interaction energies of pancake vortices. The interlayer interaction energy $U_{int,\,J}$, being field and temperature dependent, determines the degree of coupling of vortices into the third dimension perpendicular to the CuO-layers. As a consequence, not only high operating temperatures can lead to a thermal decoupling [1,2], but also high magnetic fields may result in a magnetic decoupling if the intralayer repulsion energy overcomes the interlayer coupling energy [1,3]. An even more complex situation evolves in the presence of pinning. In this case, the competition between the pinning energy U_{pin} and the intralayer interaction energy $U_{int,\,2D}$ determines whether the vortices (either pancakes or lines) behave independently or collectively.

A line which has played a tremendous role over the years in the development of ideas on the vortex dynamics in HTSC is the so-called irreversibility line (IL). Above the IL, that is in the limit of high temperatures and/or fields, the vortex system is melted and forms a liquid, while below the IL it forms a solid. Strong structural disorder of a sample, as in thin films, leads to a continuous second order phase transition at $T = T_g$ with a vortex glass (VG) phase at low temperatures leading to an exponential decay of the positional order and subohmic dynamics [4]. Close to this second order VG transition, the electric field E and current density j should scale with $|T - T_g|$, leading Fisher to postulate a scaling ansatz $E(j) \propto f_{\pm}(j)$ with the scaling functions $f_{\pm}$ [5]. For isotropic HTSC systems, a 3D scaling with a finite VG transition temperature T_g has been predicted and successfully applied to YBaCuO films [6]. For more anisotropic, layered HTSC in moderate fields a modified scaling was proposed by Yamasaki *et al.*, keeping a finite T_g in combination with a 2D scaling

[a] e-mail: `paul.ziemann@physik.uni-ulm.de`

formula to explain their data on BiSrCaCuO crystals [7]. This scaling approach was reported to be successful also for YBaCuO/PrBaCuO superlattices [8] and recently for Tl-2212 thin films [9].

The VG theory and the weak collective pinning theory (WCPT) predict for the activation barrier for flux creep $U(j)$ an algebraic decay as given by

$$U(j) = \frac{U_c}{\mu}\left[\left(\frac{j_c}{j}\right)^{\mu} - 1\right], \tag{1}$$

where U_c, j_c and μ denote the activation barrier $U(T \to 0\ \mathrm{K})$, the current density $j(T \to 0\ \mathrm{K})$ and the creep exponent $0 < \mu < 2$, respectively. For strongly anisotropic, layered HTSC within the single pancake regime, $U(j)$ is expected to saturate for decreasing currents, since there is no extra deformation energy needed to overcome barriers [10].

Only very few experiments focus on the low-H/high-T regime, because it is difficult to establish the critical-state inside the whole sample for very low fields and because of the fast relaxation of the magnetization. In this paper we experimentally study this low-H/high-T regime of the H-T phase diagram of a strongly anisotropic HTSC system by analyzing the temperature dependence of the critical current density and the temporal relaxation of the magnetic moment in a ring-shaped $Tl_2Ba_2CaCu_2O_8$ thin film in its remanent state with a SQUID allowing to extract data over 5 decades in the electric field E down to extremely low values of 10^{-16} V/cm. It will be demonstrated for these Tl-based thin films with pointlike disorder that with increasing temperature T implying a decreasing current density j, a crossover is observed from 2D pinned single vortex to quasi-2D collective creep with reduced dissipation with each of these regimes exhibiting a different $U(j)$. The fact that a coupling of the diluted vortex matter sets in at high temperatures is proposed to be due to a process similar to variable range hopping (VRH) of vortices with a hopping distance, which increases for decreasing currents and leads to an enhanced shear interaction as compared to the pinning energy.

2 Experiment

The preparation of $Tl_2Ba_2CaCu_2O_8$ thin films is performed in two steps. First a precursor film is deposited on a (001) $LaAlO_3$ substrate by means of dc sputtering from the Tl:Ba:Ca:Cu = 2:2:1.2:2 target. Then this film is annealed in pure argon atmosphere at 770 °C for about 6 h. Details on this preparation process were described elswhere [11]. The data reported here were observed on a 2 300 Å thick film with a resistively measured zero resistance transition temperature of $T_{c,0} = 105$ K and a transition width of $\Delta T_c \cong 4$ K. X-ray diffraction patterns (XRD) revealed (00l) peaks only indicating a highly textured film growth. For patterning ring shaped samples, wet chemical etching with H_3PO_4 was used. The resulting ring has an outer diameter of $d = 2$ mm and a width of $w = 27\ \mu$m. Accordingly, a d/w ratio of 74 is obtained,

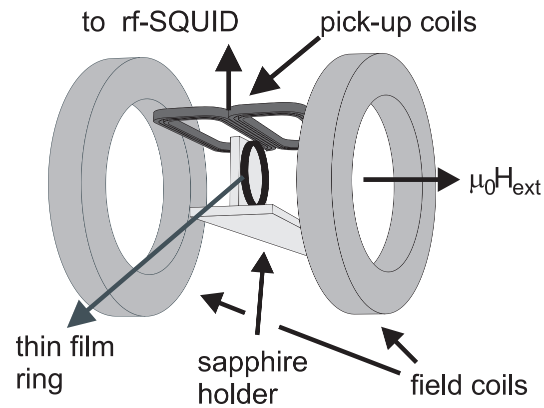

Fig. 1. Experimental setup located in vacuum including superconducting field coils, sapphire sample holder onto which the thin film ring is mounted, and superconducting pick-up coils connected to a *rf*-SQUID immersed in LHe. All parts are thermally coupled *via* sapphire parts to the bottom of a LHe cryostat.

which fulfills the condition $d/w > 20$ for an ideal narrow ring, as has been shown by Herzog *et al.* [12].

A specially designed *rf*-SQUID magnetometer is used for detecting magnetic signals (resolution 10^{-8} emu) of thin films with a sapphire sample holder mounted onto the bottom of a LHe cryostat in vacuum while the SQUID-head is immersed inside the cryostat in LHe. The sample is surrounded by a superconducting Nb cylinder and additional mu-metal sheets for magnetic shielding. As can be seen from Figure 1 the sample itself is mounted on top of a sapphire lever and can be moved *in situ* into the gap between a pair of 1 T NbTi-coils in Helmholtz geometry. The pick-up coils forming a planar gradiometer arrangement were located just above the sample perpendicular to the field coils. The following procedure was applied in all cases for determining the relaxation behavior. The ring shaped thin film is first field cooled (FC) to the target temperature $T < T_c$ (10 K$\ldots$93 K) in a magnetic field of $H = 100$ Oe parallel to the c-axis. The temperature stability was better than 10 mK. Then, the magnetic field is quenched inducing a circulating current inside the ring. The corresponding magnetic moment is detected by the SQUID and monitored for 2 000 s. After this time, the sample is heated to above T_c allowing to determine the residual magnetization at T after the relaxation process. From a knowledge of the inductance L of the ring [13], the current $I(t)$ can be calculated from the magnetic moment. Its time derivative gives the electric field E according to $E = -(L/\pi d) \cdot dI(t)/dt$ and after elimination of time, the E-j characteristics are obtained. This type of measurement was first suggested by Sandvold and Rossel [14].

An additional note may be in order. The high sensitivity of the SQUID measurements, however, is also the source of an experimental problem. Any drift induced in the SQUID system by *e.g.* creeping of an externally applied magnetic field, significantly deteriorates the measurement or even makes it impossible. To avoid this problem, the above described remanent mode was preferred, which, however, implies a principle difficulty in the interpretation of the experiment. This has to do with the changing magnetic induction during relaxation measurements, while standard procedures to extract physical properties demand isothermal measurements under a constant magnetic field. As will be shown, it is the combination of the ring geometry of our samples with remanent measurements at high temperatures and small fields, which allows to extract meaningful conclusions from remanent relaxation experiments.

For an estimate of the magnetic field and the corresponding induction B one has to take into account three contributions, the B_{rem} itself, the magnetization due to the induced currents B_{self} and the ambient field. It is a characteristic property of an ideal ring to show a hysteresis loop shaped like a parallelogram [15]. Accordingly, the ZFC and remanent signal *vs.* temperature should show symmetric behavior with no FC response, a feature which can be seen in the present ring sample, indicating that B_{rem} can be neglected. Furthermore, our ring shaped samples have a large diameter/width ratio resulting in currents induced by switching off a 100 Oe field, which by far exceed the critical current density even at the lowest temperature of 10 K. Therefore, these currents are not able to freeze in the entire cooling field. It turns out (*cf.* Sect. 3.1) that for temperatures above 55 K the earth magnetic field component of 0.2 Oe becomes the relevant constant external field, while for lower temperatures changes of the self-field due to the current relaxation of the order of only 1 gauss have to be taken into account. One should recall that dissipation arises due to flux quanta Φ_0 transversing the ring material from inside driven by a radial field gradient. Due to their radial movement through the ring material electric fields are created resulting in dissipation. Thus, for the process of flux quanta transversing the ring it should still be possible to apply the flux creep formalism.

3 Results and discussion

3.1 Critical current density

The ring shaped sample is first zero-field-cooled (*i.e.* ambient field) to $T = 5$ K and then a field H with 0.03 Oe $\leq H < 30$ Oe is applied inducing a macroscopic shielding current in the ring. Next, the temperature of the sample is increased and the corresponding ring moment is monitored. An example for such a measurement is given in Figure 2 for a field $H = 0.14$ Oe parallel to the *c*-axis. The magnetic signal retains its starting value up to a well defined temperature T^*, where the magnitude of the signal starts to decrease. At T^* the induced current density $j(5\text{ K})$ corresponds to the critical value $j_c(H, T^*)$. Thus, for $T > T^*$ from the experimental curve the temperature dependence of $j_c(T)$ can be extracted if the inductance L of the ring is known. In the following, L is calculated

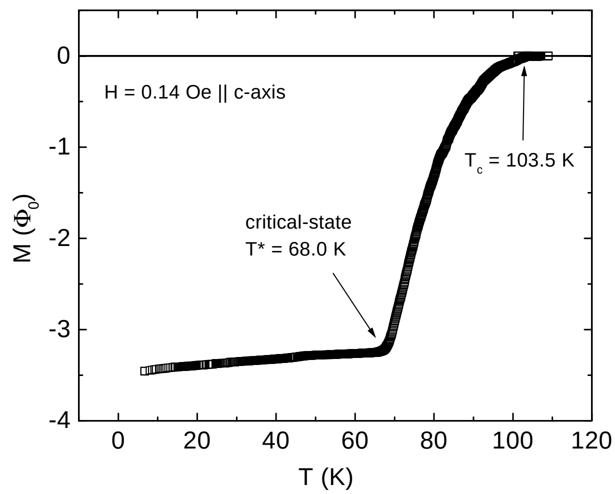

Fig. 2. Temperature dependence of the magnetic signal of a Tl-2212 ring (diameter 2 mm, width 27 μm) induced by applying a field $H = 0.14$ Oe after ZFC to 5 K as determined by a SQUID. The induced supercurrent density reaches its critical value j_c at T^*, above which the critical-state inside the ring material is established with a density $j_c(T)$ until, at T_c, superconductivity vanishes.

from [13]

$$L = \mu_0 \bar{R} \left[\ln \left(\frac{8\bar{R}}{w} \right) - \frac{1}{2} \right], \quad (2)$$

where $\bar{R}$ is the mean radius and w the width of the ring. Eventually, as can be seen from Figure 2, by further increasing the temperature, at $T = T_c = 103.5$ K the transition into the normal state is approached, where the magnetic signal vanishes. This result demonstrates, on the other hand, that switching-off a field of $H = 0.14$ Oe would induce currents allowing to freeze in the entire field at low temperatures. We find that T^* shifts to a value below 10 K for $H > 1.3$ Oe. This means that quenching in $H = 100$ Oe yields a current density, which immediately decays to a corresponding self-field $B_{self} \sim 1.3$ G, while the effective component of the earth field sets the lower limit of $\mu_0 H = 0.2$ G.

To further analyze $j_c(T)$, the data are plotted in the form $\log(j)$ *vs.* $\log[1-(T/T_c)]$, since for the standard power law $j_c(T) \propto [1 - (T/T_c)]^\alpha$, which is expected to hold at least close to T_c, this representation immediately delivers the exponent α. Applying this procedure to a ring patterned ($d = 1$ mm, $w = 50$ μm), 200 nm thick YBaCuO film ($T_c = 90.7$ K) gives the result shown in the inset of Figure 3. Here, a straight line is observed with a slope of $\alpha = 1.3$ confirming previous results on this material [16, 17]. This standard behavior found for YBaCuO is in contrast to the results found for Tl-2212 rings presented in the main panel of Figure 3. Clearly, the temperature dependence in this case exhibits a kink at $T_k = 96.3$ K. Above and below T_k, the data can be reasonably well approximated by straight lines with different slopes of $\alpha = 2.0$ and 1.0, respectively. This change of slopes indicates that the critical current density above T_k is much

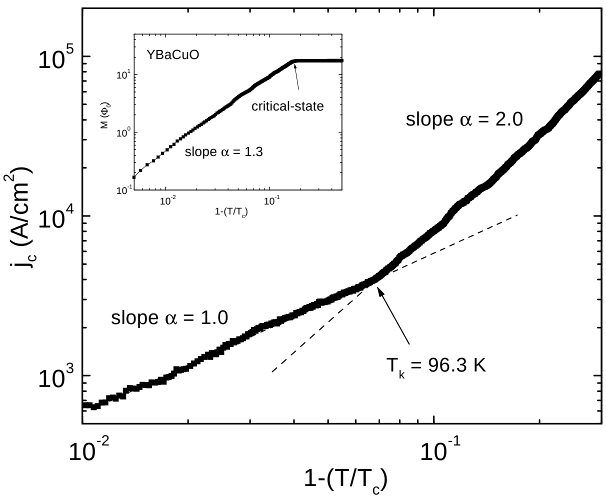

Fig. 3. Double logarithmic plot of the critical current density j_c *vs.* $(1 - T/T_c)$. At $T_k = 96.3$ K a significant change of slope from $\alpha = 2.0$ to $\alpha = 1.0$ is visible denoting a smaller j_c-decrease than what is extrapolated from low temperatures (dashed lines). The inset shows corresponding data for a YBaCuO thin film ring ($d = 1$ mm, $w = 50$ μm, $T_c = 90.7$ K). Here no kink is seen in contrast to the Tl-2212 ring with its high intrinsic anisotropy.

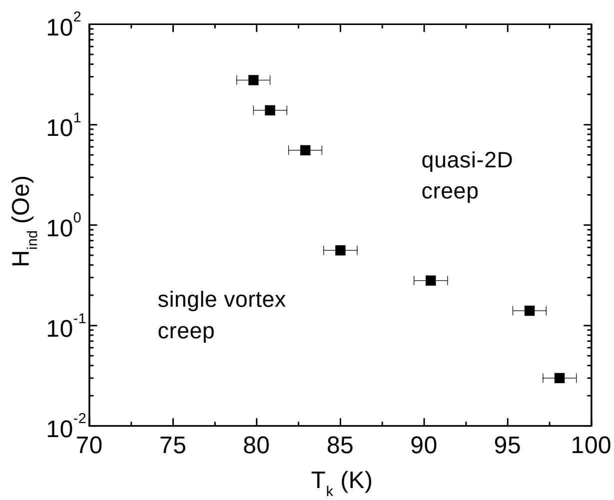

Fig. 4. H-T "phase" diagram constructed from the temperature T_k and the corresponding field Hind for various fields 0.03 Oe $\leq H < 30$ Oe. The error bars reflect the uncertainty in determining T_k. This borderline represents the crossover from single vortex to quasi-2D collective creep when increasing the temperature as discussed in the text. Note the beginning of saturation for $H_{ind} < 0.2$ Oe $= H_{Earth}$ at a constant T.

less depressed by increasing the temperature than what is expected by extrapolating from below T_k, *i.e.* dissipation becomes smaller. The temperature T_k is found to depend on H_{ind}, the field switched on to induce the supercurrents in the ring, which also remains applied during the measurement. This allows to construct a H_{ind}-T_k boundary curve as presented on log-lin-scales in Figure 4.

It is tempting to interpret the kink in $j_c(T)$ as being related to a current dependent length scale for the interaction of pancake vortices, which, to explain the observed anomaly, would have to increase for increasing temperatures to allow a stronger interaction resulting in a more sluggish dynamics when approaching T_c. In the next chapter the dynamics of these two regimes, below and above T_k, will be identified, thereby suggesting a crossover from single vortex to collective creep, which is triggered by the decreasing current.

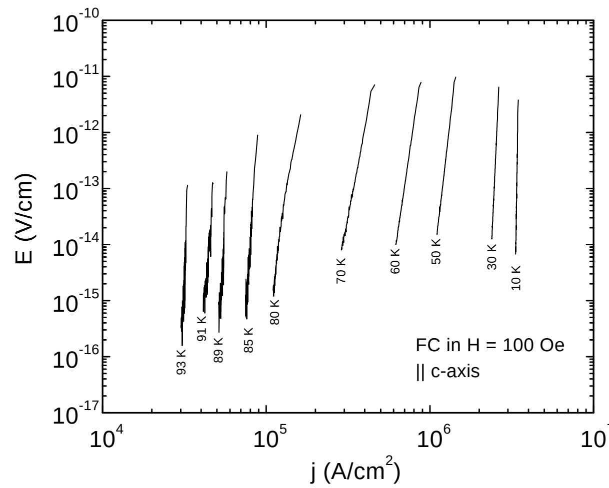

Fig. 5. Current-voltage isotherms of a Tl-2212 film determined from temporal relaxation measurements on a remanent state prepared by FC in 100 Oe and switching off the field (a SQUID technique is applied). Note the extremely low electric fields for higher temperatures accessible due to the SQUID technique.

3.2 Magnetic relaxation

In Figure 5 isothermal E-j characteristics are presented as extracted from the temporal relaxation of the remanence of a Tl-2212 thin film ring after FC in $H = 100$ Oe parallel to the c-axis. Note the small values of E, which, in the present geometry, correspond to voltages of the order of 10^{-16} V demonstrating the high sensitivity of the experimental technique. For increasing temperatures, from 10 K to 80 K the characteristics become more flat as expected, while for even higher temperatures above 80 K the slopes increase again signaling lower dissipation within the material of the ring.

To analyze the temporal decay of the ring current $j(T, t)$ in more detail, we refer to the corresponding normalized relaxation rate S as given by Geshkenbein *et al.* [18]

$$S \equiv -\frac{d \ln[j(T,t)]}{d \ln(t)} = \frac{k_B T}{U_c(T) + \mu k_B T \ln(t/t_0)}, \qquad (3)$$

where U_c denotes the temperature dependent activation energy, μ the glassy exponent and t_0 a logarithmic time scale. In Figure 6, the temperature dependence of the relaxation rate $S(T)$ is presented as taken at 100 s after quenching the magnet (solid symbols). The relaxation rate starts with the small value of 0.5% at $T = 10$ K and

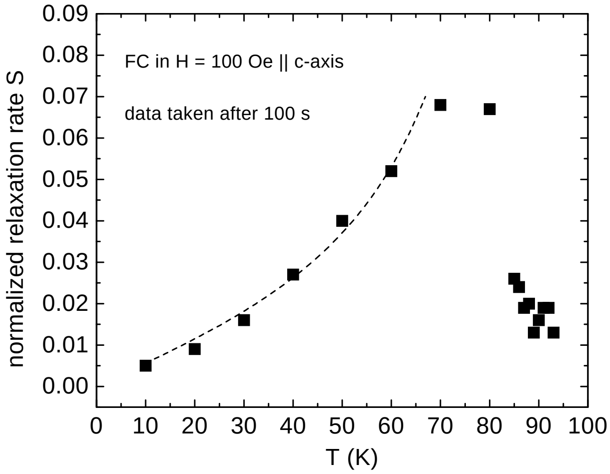

Fig. 6. Normalized relaxation rate $S = -d\ln(j)/d\ln(t)$ determined at $t = 100$ s after switching off the field $H = 100$ Oe used for FC. The dashed line is a fit with equations (3, 4a) for 10 K $\le T \le$ 60 K with $U_c(0) = 156$ meV. For temperatures $T > 80$ K, the sharp drop in S indicates a suppressed dissipation which is attributed to a single vortex to quasi-2D crossover.

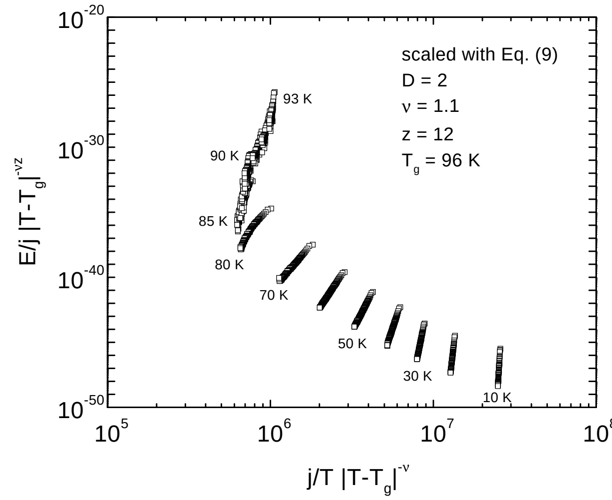

Fig. 8. E-j characteristics (from Fig. 5) scaled according to the so-called quasi-2D VG theory with equation (9) and $D = 2$. The scaling of the $T > 80$ K data yields reasonable exponents $z = 12$ and $\nu = 1.1$. The data for $T < 80$ K, where 2D pinned single vortex dynamics is expected, do not follow the quasi-2D scaling.

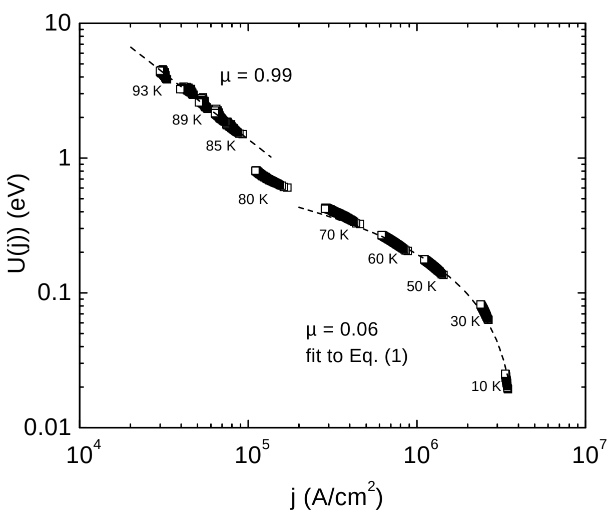

Fig. 7. Current dependence of the activation barrier $U(j)$ on a double-logarithmic scale. For $T > 80$ K a matching constant $C = 55$ was used instead of $C = 40$. For the two temperature regimes 10 K $\le T \le$ 60 K and 85 K $\le T \le$ 93 K exponents μ are extracted as given in the figure resulting in the 2 dashed lines. A discussion of these values is given in the text.

smoothly increases to 6.8% at $T = 70$ K. For temperatures $T > 80$ K, Figure 6 reveals a sharp drop of S approaching an almost constant value $S \approx 1.7\%$, indicating the above mentioned lower dissipation. It signals the onset of a different type of dynamics for temperatures above 80 K as compared to the behavior for $T \le 70$ K. A possible interpretation of these different regimes of dynamics is the main topic of the following part of this paper.

We start with analyzing the low temperature data of Figure 6. For this purpose, some results have to be anticipated, which will be discussed in detail below. First, from a scaling analysis of E-j curves (*cf.* Fig. 8) it is concluded that the vortices form a 3D vortex glass below $T_g = 96$ K. Second, from a Maley analysis (*cf.* Fig. 7), a very small μ value of 0.06 is obtained for the low-T regime within 10 K... 70 K. Such small μ-values, reflecting a logarithmic $U(j)$-dependence, have been found before in highly anisotropic HTSC, like Tl-2212 and Bi-2212 [19–22] at low temperatures. Thus, in equation (3) the second term in the denominator $[\mu T \ln(t/t_0)]$ is significantly smaller than $[U_c(T)/k_B]$ at low temperatures and can be neglected. Furthermore, assuming 2D vortex pinning (see estimate of L_c below) as the dominant mechanism, $U_c(T)$ can be estimated in the following way. Depending on whether δl- or δT_c-pinning is relevant, corresponding expressions for $U_c(T)$ have been reported by Wen *et al.* [23], which read for the present 2D case

$$\delta l: \quad U_c(t) = U_c(0)(1-t^2)^{3/2}(1+t^2)^{1/2} \qquad (4a)$$

$$\delta T_c: \quad U_c(t) = U_c(0)(1-t^2)^{1/2}(1+t^2)^{3/2}, \qquad (4b)$$

with $t = T/T_c$ the reduced temperature. Thus, the modified equation (3) together with equations (4) provide all ingredients to describe the low temperature data of Figure 6 with $U_c(0)$ being the only fitting parameter. The dashed line in Figure 6 represents the result of such a fitting procedure for δl-pinning with $U_c(0) = 156$ meV giving a good description of the data. It is important to note that by using equation (4b), *i.e.* δT_c-pinning, one is not able to obtain a reasonable fit to the experimental results. Thus, at this point it is concluded that the observed increase of the relaxation rate for increasing temperatures $T \le 70$ K can be attributed to creep of 2D δl-pinned single vortices, exhibiting a pancake behavior due to the high anisotropy in our samples as opposed to the more isotropic YBaCuO.

According to Maley *et al.* it is possible to determine the activation barrier for vortex motion $U(j)$ directly from the relaxation data $j(t)$ by using [24]

$$U(j,0,H) = -k_B T \left[\ln\left(\frac{dj}{dt}\right) - C \right] g^{-1}(T). \qquad (5)$$

The constant C contains the magnetic induction and all macroscopic properties such as the sample dimension, whilst $g(T)$ contains the (separated) temperature dependence according to $g(T) = [1-(T/T_c)^2]^{3/2}$. The possibility of such a separation was experimentally confirmed on YBaCuO thin films by Xiao *et al.* [25].

To get a smooth master curve one has to take two different C's, for $T < 80$ K a value of 40 is needed, while for $T > 80$ K a value of 55 matches the individual relaxation curves as can be seen in Figure 7 on double-log scales. This different scaling behavior for $T > 80$ K is a further hint to a crossover in vortex dynamics. These two dynamic regimes become even more clear by describing the extracted current dependence of $U(j)$ in terms of weak collective pinning theory. There are two distinct regimes clearly visible: (i) for 10 K $\leq T \leq$ 70 K, the corresponding exponent is $\mu = 0.06$ (dotted line in Fig. 7), while (ii) for $T \geq 85$ K (low current regime) the exponent μ can be deduced directly from the slope in the double-log plot of Figure 7, since $j \ll j_c$, *i.e.* $\log[U(j)] \propto -\mu \log(j)$ which yields $\mu = 0.99$.

According to the WCPT, the effect of pinning by randomly distributed weak pinning centers leads to a finite correlation lengths L_c parallel and perpendicular to the external magnetic field. Thus, in the parallel case vortex segments of this length can be assumed to be pinned independently. Since in our experiment, the magnetic field is aligned parallel to the c-axis, the appropriate length reads [10]

$$L_c^c \cong \varepsilon \xi_{ab} \sqrt{\frac{j_0}{j_c}}, \qquad (6)$$

with the anisotropy factor $\varepsilon < 1$ and the depairing current density $j_0 = c\Phi_0/(12\sqrt{3}\pi^2\lambda^2\xi)$. Taking the corresponding coherence length $\xi_{ab}(0) = 25$ Å, the penetration depth $\lambda_{ab}(0) = 2\,520$ Å, $j_c(0) \approx 5 \times 10^6$ A/cm^2 and $\varepsilon = 0.01$, one gets $L_c^c(T = 0\ \mathrm{K}) = 0.9$ Å, which is smaller than the distance of CuO_2-bilayers $d = 15$ Å and indicates 2D pinning. A comparison between the pancake pinning energy U_{pc}

$$U_{pc} = \left(\frac{\Phi_0}{4\pi\lambda_{ab}}\right)^2 d \left(\frac{j_c}{j_0}\right) \qquad (7)$$

and the intralayer coupling energy $U_{int,\ 2D}$

$$U_{int,\ 2D} = \left(\frac{\Phi_0}{4\pi\lambda_{ab}}\right)^2 d \left(\frac{\xi_{ab}}{2a_0}\right)^2, \qquad (8)$$

yields $U_{int,\ 2D} < U_{pc}$, which means that single vortex (pancake) dynamics should be observed. The applicability of WCPT is, however, in conflict with our experimental observations, since it cannot explain the experimentally seen anomaly of a decreasing relaxation rate S at high temperatures $T > 80$ K (*cf.* Fig. 6).

A similar discrepancy has been reported some time ago by van der Beek *et al.* [23]. They measured the relaxation of the magnetic moment of Bi-2212 single crystals in fields between 0.1 T and 12 T. Based on WCPT they implied single pancake behavior, but the expected saturation of $U(j)$ for decreasing currents has not been found. Later, this inconsistency was emphasized by Blatter *et al.* [10], who suggested the concept of variable range hopping (VRH) [26,27] for obtaining a coupling of the pancakes to form a 2D elastic manifold. The basic idea is to substitute the coherence length ξ_{ab} in the expression for the intralayer coupling $U_{int,\ 2D} = c_{66} d \xi_{ab}^2$ by a current dependent long distance jump scale $u(j)$ according to $U_{int,\ 2D} = c_{66} d u^2(j)$, with $u(j) = \xi_{ab}(j_{pc}/j)^{1/3}$ (j_{pc} is the pancake depinning current density, c_{66} is the shear modulus). This means that for decreasing j the pancakes will couple to each other when the shear energy is of the order of the pinning energy and creep proceeds *via* the activation of "pancakes bundles" (2D collective creep).

In the present case we attribute the peak in $S(T)$ at $T = 80$ K to a crossover from 2D pinned single vortex dynamics at lower temperatures (corresponding to high currents j) to quasi-2D collective creep, where the coupling of layers is weakened due to high temperatures, while pancake vortices couple to each other and creep becomes more sluggish with $\mu \cong 1$. The theoretical value originally given by Feigel'man *et al.* for the 2D case is $\mu = 9/8$ [3] being very close to the observed one. This theoretical value, however, was questioned later by Blatter *et al.* [10] and Vinokur *et al.* [28], who obtained $\mu = 7/4$ and $1/2 \leq \mu \leq 7/4$ depending on pancake bundle sizes, respectively. To test whether this increase in μ can be attributed to a movement of 3D vortex bundles or rather to (quasi-)2D collective creep, the scaling behavior of the E-j curves according to VG theory is analyzed.

3.3 Scaling analysis

In this section a scaling analysis of the E-j characteristics is performed on the basis of VG theory [4]. Starting from the divergencies at a finite glass temperature T_g of the static coherence length $\xi_{VG}(T) \propto |T - T_g|^{-\nu}$ and the dynamic relaxation time $\tau_{VG}(T) \propto |T - T_g|^{-\nu z}$ with critical exponents ν and z, scaling laws can be deduced for the electric field E and current density j yielding [6]

$$E(j) \propto j|T - T_g|^{-\nu(D-2-z)} f_{\pm}\Big(j|T - T_g|^{-\nu(D-1)}/T\Big), \qquad (9)$$

where $f_{\pm}$ represents a two-branched universal function and D stands for the dimensionality of the problem. A modification of equation (9) was proposed by Yamasaki *et al.* for the interpretation of their E-j characteristics measured on BiSrCaCuO thin films in a magnetic field $B = 2$ T parallel to the c-axis. By taking the original formula they obtained the unphysical exponents $z = 12.2$ and $\nu = 0.69$ [7]. Taking, however, $D = 2$ in equation (12) leading to the so-called *quasi*-2D *scaling*, they obtained the more reasonable values $z = 5.61$ and $\nu = 1.38$. The idea behind this reduced dimensionality is the concept of quasi-decoupled CuO_2-bilayers with the consequence that only the in-plane correlation length $\xi_{ab} \propto |T - T_g|^{-\nu}$ is of relevance, whereas ξ_c (parallel to the c-axis) is substituted by the temperature independent interlayer distance.

In the present work on Tl-2212 films in very low magnetic fields, by using the modified equation (9) we obtain the critical exponents $\nu = 1.1$, $z = 12$ and a finite glass temperature of $T_g = 96$ K, as can be seen in Figure 8. It is important to note that only the data above 80 K, which according to the last section are expected to exhibit collective behavior can be scaled. This corroborates the conclusion of the last section that there are two regimes of completely different vortex dynamics, namely single vortex (pancake) and quasi-2D at low and high temperatures, respectively. The situation concerning the dimensionality of the observed vortex dynamics is far from clear cut even for identical systems like Tl-2212, showing either 3D [29] and quasi-2D [9]. It may well be that a decision whether a 3D or quasi-2D description is more appropriate hinges on sample anisotropy. The value of $z = 12$ as deduced from our quasi-2D scaling appears relative high, yet not unreasonable if compared to other values reported previously. For example, z values of up to 10 have been found previously for Tl-2212 as well as for YBaCuO thin films [30–32]. There seems to be a tendency towards high z values for very low magnetic fields or small sample dimensions.

Interestingly, Zavaritsky *et al.* measured the temporal decay of the remanent state in Tl-2212 single crystals and found an anomalous decrease in the normalized relaxation rate S closely resembling that reported here occuring, however, at the much lower temperature $T = 23$ K [33]. They interpret the drop in $S(T)$ as a crossover from single vortex creep to a creep of vortex bundles. Nideröst *et al.* report a similar anomaly in $S(T)$ observed by relaxation measurements on the remanent state of Bi-2212 single crystals [22]. From WCPT they suggest a crossover from single pancake to vortex bundle creep. One has to distinguish, however, between vortex dynamics in crystals and films, since the presence of the so-called fishtail peak in the former generates a decrease in $S(T)$, too [34]. Miu *et al.* measured transport properties of Bi-2212 *thin films* without external magnetic fields and close to T_c [35]. Within a small temperature range around 78 K, from their I-V-characteristics a decreasing relaxation rate S is deduced for increasing T-values while for even higher temperatures S increases again. These authors interprete their observation as being due to a crossover from completely decoupled 2D layers to quasi-2D behavior with a finite coupling and eventually to pure 2D again. The 2D behavior at high T is attributed to thermal decoupling, the intermediate quasi-2D part to a finite Josephson coupling which vanishes for $T < 78$ K, since then the Josephson length given here by $\lambda_J = d/\varepsilon$ exceeds the relevant probing length r_c. An estimate of r_c for our present case yields a value $r_c \approx 5$ μm, which by far exceeds $\lambda_J = 150$ nm (for this estimate the following parameters were assumed: $T = 80$ K, the slope of the characteristic $\alpha \cong 10$, the spacing between the bilayers $d = 15$ Å and the current density at the anomaly $j = 1 \times 10^5$ A/cm^2 (*cf.* Fig. 5)). Obviously, the matching of length scales $\lambda_J \approx r_c$ necessary for the above scenario of a quasi-2D/2D crossover is not fulfilled in the present case.

There is another important scenario of vortex dynamics in highly anisotropic HTSC for the case of vanishing external fields and elevated temperatures, where the bilayers can be considered as being decoupled, namely the Berezinskii-Kosterlitz-Thouless (BKT) picture [36, 37]. Within this theory dissipation is generated by thermally excited 2D vortex/antivortex pairs, which for $T < T_{BKT} < T_c^{MF}$ are logarithmically bound and do not contribute to a finite resistivity. At T_{BKT}, however, the pairs dissociate and produce a measurable voltage. For an applied current the pairs dissociate even below T_{BKT} leading to a power-law behavior of I-V-characteristics according to $E \propto j^{\alpha(T)}$ with an universal jump of α from 3 to 1 at T_{BKT}. Such a transition has been reported recently to occur in Tl-2212 thin films for $\mu_0 H = 0$ T at a temperature $T_{BKT} = T_c(\rho = 0) = 103.7$ K with $T_c^{MF} = 109$ K [9]. From the temperature dependence of $\alpha(T)$ it is found that for $T < 93$ K a deviation from the theoretical BKT behavior occurs pointing to the development of finite Josephson coupling between adjacent bilayers. Interestingly, $T = 93$ K is the highest possible temperature for measuring current decay within the present work. This can then be understood by assuming that in the true 2D case dissipation is large, leading to a fast (1–2 s) decay of the induced current below the resolution limit of the apparatus before taking the first data point.

4 Conclusion

Tl-2212 films were studied with respect to the temperature dependence of the critical current density $j_c(T)$, thereby revealing an anomaly with reduced dissipation for increasing temperature and allowing to construct a H-T borderline. Such an anomaly cannot be explained by standard collective pinning theory, which predicts in our case single vortex (pancake) dynamics over the whole temperature range. From additionally determined normalized relaxation rate behavior $S(T)$ one concludes on two different regimes of dynamics starting with a 2D pinned single vortex behavior at low temperatures ($T < 80$ K) crossing over to a plateau-like regime with reduced dissipation at high temperatures ($T > 80$ K). The decreased relaxation rate is attributed to an enhanced value of μ as consistently determined from the Maley-procedure. To extract the relevant dimensionality of the vortex dynamics in the high temperature regime, scaling analysis were performed pointing to quasi-2D collective creep. For the underlying mechanism leading to a coupling of pancace vortices at high temperatures, corresponding to low current densities, a hopping process of vortices is suggested with a current dependent hopping distance as has been used for variable range hopping (VRH).

This work was supported by the Deutsche Forschungsgemeinschaft. One of us (H.H.W.) would like to thank the Alexander von Humboldt Stiftung for financial support. We are grateful to Professor S.L. Yan's group at Nankai University, Tianjing, P.R. China, for providing the Tl-2212 films.

References

1. L.I. Glazman, A.E. Koshelev, Phys. Rev. B **43**, 2835 (1991).
2. A. Schilling, R. Jin, J.D. Guo, H.R. Ott, Phys. Rev. Lett. **71**, 1899 (1993).
3. M.V. Feigel'man, V.B. Geshkenbein, A.I. Larkin, Physica C **167**, 177 (1990).
4. M.P.A. Fisher, Phys. Rev. Lett **62**, 1415 (1989).
5. D.S. Fisher, M.P.A. Fisher, D.A. Huse, Phys. Rev. B **43**, 130 (1991).
6. R.H. Koch, V. Foglietti, W.J. Gallagher, G. Koren, A. Gupta, M.P.A. Fisher, Phys. Rev. Lett. **63**, 1511 (1989).
7. H. Yamasaki, K. Endo, S. Kosaka, M. Umeda, S. Yoshida, K. Kajimura, Phys. Rev. B **50**, 12959 (1994).
8. B. Zhao, F. Ichikawa, T. Fukami, T. Aomine, J.J. Sun, B. Xu, L. Li, Phys. Rev. B **55**, 1247 (1997).
9. H.H. Wen, P. Ziemann, H.A. Radovan, S.L. Yan, Europhys. Lett. **42**, 319 (1998).
10. G. Blatter, M.V. Feigel'man, V.B. Geshkenbein, A.I. Larkin, V.M. Vinokur, Rev. Mod. Phys. **66**, 1125 (1994).
11. S.L. Yan, L. Fang, Q.X. Song, J. Yan, Y.P. Zhu, J.H. Chen, S.B. Zhang, Appl. Phys. Lett. **63**, 1845 (1993).
12. T. Herzog, H.A. Radovan, P. Ziemann, E.H. Brandt, Phys. Rev. B **56**, 2871 (1997).
13. J. Gilchrist, E.H. Brandt, Phys. Rev. B **54**, 3530 (1996).
14. E. Sandvold, C. Rossel, Physica C **190**, 309 (1992).
15. E.H. Brandt, Phys. Rev. B **55**, 14513 (1997).
16. J.W.C. de Vries, M.A.M. Gijs, G.M. Stollman, T.S. Baller, G.N.A. van Veen, J. Appl. Phys. **64**, 426 (1988).
17. V.S. Bobrov, M.A. Lebyodkin, Physica C **178**, 411 (1991).
18. V.B. Geshkenbein, A.I. Larkin, M.V. Feigel'man, V.M. Vinokur, Physica C **162-164**, 239 (1989).
19. M. Nideröst, A. Suter, P. Visani, A.C. Mota, G. Blatter, Phys. Rev. B **53**, 9286 (1996).
20. C.J. van der Beek, P.H. Kes, M.P. Maley, M.J.V. Menken, A.A. Menovsky, Physica C **195**, 307 (1992).
21. L. Ammor, A. Smina, J.C. Soret, A. Ruyter, V. Ta Phuoc, B. Martinie, J. Lecomte, B. Mercey, C. Simon, Physica C **273**, 281 (1997).
22. H.H. Wen, R.L. Wang, H.C. Li, B. Yin, S.Q. Guo, Z.X. Zhao, S.L. Yan, L. Fang, M.S. Si, Phys. Rev. B **54**, 1386 (1996).
23. H.H. Wen, H.G. Schnack, R. Griessen, B. Dam, J. Rector, Physica C **241**, 353 (1995).
24. M.P. Maley, J.O. Willis, H. Lessure, M.E. McHenry, Phys. Rev B **42**, 2639 (1990).
25. Z.L. Xiao, J. Häring, C. Heinzel, P. Ziemann, Solid State Comm. **95**, 153 (1995).
26. N.F. Mott, Philos. Mag. **19**, 835 (1969).
27. B.I. Shklovskii, A.L. Efros, *Electronic Properties of Doped Semiconductors, Springer Series in Solid-State Sciences* N° 45 (Springer, Berlin, 1984).
28. V.M. Vinokur, P.H. Kes, A.E. Koshelev, Physica C **248**, 179 (1995).
29. V. Ta Phuoc, A. Ruyter, L. Ammor, A. Wahl, J.C. Soret, C. Simon, Phys. Rev. B **56**, 122 (1997).
30. H.C. Li, J.W. Li, R.L. Wang, B. Yin, Z.X. Zhao, S.L. Yan, L. Fang, M.S. Si, Physica C **246**, 330 (1995).
31. Y. Ando, H. Kubota, S. Tanaka, Phys. Rev. Lett. **69**, 2851 (1992).
32. T. Nojima, T. Ishida, Y. Kuwasawa, Physica C **263**, 424 (1996).
33. V.N. Zavaritsky, N.V. Zavaritsky, Physica C **185-189**, 1887 (1991).
34. M. Reissner, J. Lorenz, Phys. Rev. B **56**, 6273 (1997).
35. L. Miu, G. Jakob, P. Haibach, T. Kluge, U. Frey, P. Voss-de Haan, H. Adrian, Phys. Rev. B **57**, 3144 (1998).
36. V.L. Berezinskii, Sov. Phys. JETP **32**, 493 (1971).
37. J.M. Kosterlitz, D.J. Thouless, J. Phys. C **6**, 1181 (1973).